THE ORIGIN OF NON-MARE MASCON GRAVITY ANOMALIES ON THE MOON. J. C. Andrews-Hanna[1], [1]Department of Geophysics, Colorado School of Mines, Golden, CO (jcahanna@mines.edu).

Introduction: Although a significant fraction the mascon gravity anomalies can be explained by the flexural support of the mare basalts within the basins, in some cases this explanation does not suffice. A number of the lunar basins exhibit mascons in excess of that which can be accounted for by the maria, and some basins possess central gravity anomalies yet lack mare fill altogether [1]. An example of a prominent non-mare mascon is found in Orientale, in which the central gravity anomaly reaches a value of ~180 mGal relative to the field outside the basin, but the mare partially covering the basin floor has a thickness less than 600 m [2]. Neglecting the flexural response to the mare loading, the maximum gravity anomaly that can arise from the mare alone is ~80 mGal. These non-mare mascons were previously interpreted as arising from the instantaneous super-isostatic rebound of the basin floor and underlying mantle plug following the impact [1, 3]. However, this mechanism would require a sufficiently thick lithosphere to exist in the moments following the impact, which would seem at odds with the excavation of the majority of the lithosphere and extreme thermal and shock weakening of the remainder. This study suggests instead that the non-mare mascons are a secondary effect of the gradual flexural rebound of a thickened annulus of sub-isostatic crust surrounding the basins [4]. This is supported by gravity observations and finite element models.

Observations: In the free air gravity, those basins that possess non-mare mascons are also surrounded by annuli of strongly negative gravity anomalies (Figure 1). These annuli likely correspond to rings of thickened yet sub-isostatic crust, originating as basin ejecta [3]. This is consistent with models of basin formation, which predict the basins and their surroundings to be left in a strongly sub-isostatic state in the after-math of the impacts [4]. These over-thick crustal roots would have acted as upward-directed loads on the lithosphere, causing flexural uplift of the annuli, which would uplift the basin center as well. Though it could be suggested that the negative gravity rings surrounding the basins arise as a result of the flexural subsidence beneath the maria, this is inconsistent with the relative magnitudes of the anomalies. The total present-day loads associated with the central mascons and surrounding negative annuli can be quantified by integrating the gravity anomaly relative to the surroundings over the area of the mascon/annulus. For three of the basins that possess significant non-mare mascons, the magnitude of the integrated negative gravity anomaly over the annulus exceeds the magnitude of the integrated positive anomaly over the mascon by factors of 5-25 (Table 1). Thus, the central mascon could plausibly be explained as an effect of the flexural uplift of the annulus together with the basin center, but the opposite scenario is not viable. In contrast, basins such as Imbrium and Serenitatis possess sufficient mare fill to explain the observed gravity anomalies and lack significant negative gravity annuli.

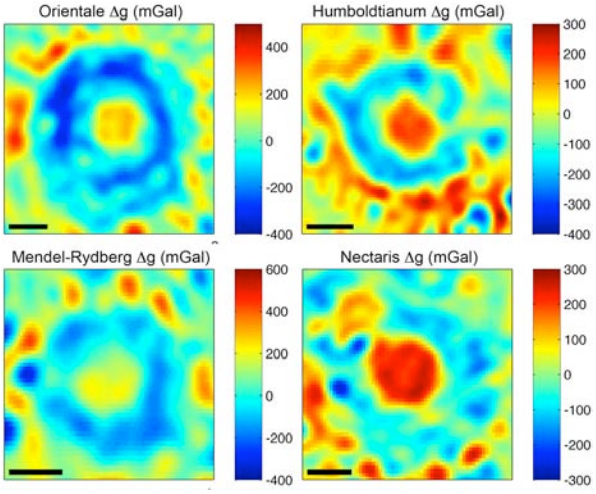

Figure 1. Free-air gravity [5] maps of lunar basins possessing non-mare mascons (scale bar is 200 km).

BASIN	$g_{annulus}$ mGal	g_{center} mGal	$g_{c,T}$ mGal km^2	$g_{a,T}$ mGal km^2	$g_{a,T}/g_{c,T}$
Orientale	-174.5	77.9	-11.5×10^{13}	0.46×10^{13}	25.1
Humboldt.	-143.7	89.4	-3.71×10^{13}	0.36×10^{13}	10.3
Mendel-Ryd.	-100.7	91.5	-2.43×10^{13}	0.47×10^{13}	5.21
Nectaris	-69.4	147.6	-2.61×10^{13}	1.77×10^{13}	1.47
Imbrium	-61.9	157.8	-7.43×10^{13}	5.82×10^{13}	1.28
Serenitatis	-60.0	198.5	-3.84×10^{13}	5.54×10^{13}	0.69

Table 1. Mean and integrated gravity anomalies within the annuli and central mascons.

Modeling: In order to test the hypothesis that the sub-isostatic annuli surrounding the basins are the cause of the non-mare mascons, the crustal structure of Orientale is first determined using azimuthally-averaged gravity and topography data to amplify the signal to noise ratio and enable higher resolution models than would otherwise be possible [4]. Both single and double-layer crust models are considered, with the double-layer models constrained such that the lower

crust remains constant in thickness except where it is excavated by the impact, with the excess crust within the thickened annulus of basin ejecta comprised of upper crustal material (Figure 2). The optimal models are expanded out to spherical harmonic degree 103, with a cosine taper applied between degrees 83-103. These models reveal an excess thickening of the crust around Orientale of ~36 and 19 km, respectively.

Spherical axisymmetric elastic finite element models [6] are then used to examine the flexural evolution of the basin. The models are initialized using the single layer crustal structure model as an initial condition, excluding the mare. The basin center is then placed in an isostatic position. The flexure is modeled for a uniform lithosphere thickness exterior to the basin (here assumed to be 60 km) and a range of lithosphere thicknesses in the basin interior (10-50 km). The lithosphere within the basin would have been reduced to zero by the impact, and then would have gradually thickened as the basin floor material cooled. The model is then iterated to find the initial condition that will result in the present-day topography and crustal thickness exterior to the basin after flexure, while the interior of the basin is always assumed to be isostatic prior to flexural uplift. This results in flexural uplift of ~2.5 km of the annulus surrounding the basin. The flexural uplift of the basin interior ranges from 1.1-2.3 km for central lithosphere thicknesses ranging from 10-50 km.

Although the gravity anomalies can be calculated directly from the models, these cannot be compared with the data. The definition of isostasy in the finite element model (equal mass in adjacent columns of rock) neglects the important effects of self-gravitation. As a result, an "isostatic" basin as defined by the finite element model would be characterized by much more strongly negative gravity anomalies than occur in nature. Rather, the change in gravity anomaly from the initial to final condition of the basin resulting from the flexure is modeled. For Orientale, central gravity highs ranging from 190 to 320 mGal are predicted when the lithosphere beneath the basin center ranges from 10-50 km thick. The larger of these anomalies greatly exceed the observed mascon of Orientale. Thus, even the presence of a thin lithosphere beneath the basin will produce a central mascon gravity anomaly during the flexural uplift of the annulus. Because the uplift of the annulus is limited by the viscous response time of the lunar mantle (likely much greater than post-glacial rebound timescales as a result of the high viscosity anhydrous lunar mantle), there is ample time for lithosphere thickening during the course of the uplift.

Conclusions: Both gravity observations and finite element models support the hypothesis that the mascon gravity anomalies in excess of those generated by the mare are a result of the flexural uplift of an annulus of thickened yet sub-isostatic crust surrounding the basins. Thus, the origin of the non-mare mascons was a gradual flexural effect, rather than an instantaneous over-shoot in the mantle rebound.

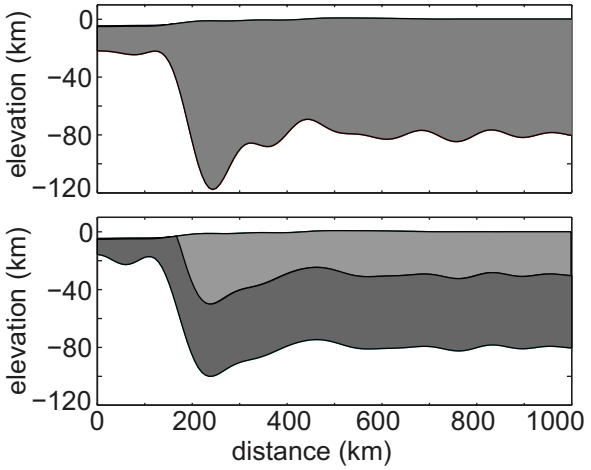

Figure 2. Single and double-layer crustal thickness models of Orientale, showing mare (black), upper crust (light gray) and lower crust (dark gray).

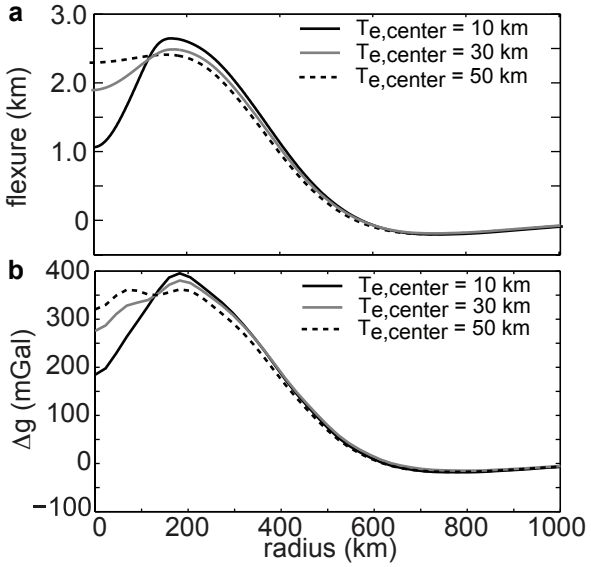

Figure 3. Predicted flexural uplift of the sub-isostatic annulus and isostatic basin floor, for lithosphere thicknesses beneath the basin center ranging from 10-50 km (**a**) and the change in gravity anomaly arising from the flexure (**b**).

References: [1] Neumann G. A., et al. (1996) *JGR 98* 17011-17028. [2] Williams K. K. and Zuber M. T. (1998) *Icarus 131* 107-122. [3] Wieczorek M. A. and Phillips R. J. (1999) *Icarus 139* 246-259. [4] Andrews-Hanna J. C. and Stewart S. T. (2011) *LPS 42* abstract 2194. [5] Mazarico E., et al. (2010) *JGR* 115, E05001, doi:10.1029/2009JE003472 [6] Melosh H. J. and Raefsky A. (1982) *Geophys. J. R. Astron. Soc. 60* 333-354.